De novo Drug Design to Suppress Coronavirus RNA-Glycoprotein via PNA-Calcitonin

Soykan Agar[1]* iD **, Barbaros Akkurt[2]** iD **, Levent Alparslan[3]** iD

[1]Kocaeli Health and Technology University, Faculty of Pharmacy, Yeniköy Mahallesi Ilıca Caddesi No:29, Başiskele/Kocaeli, Türkiye
[2]Istanbul Technical University, Faculty of Science and Letters, Department of Chemistry, Istanbul 34469, Türkiye
[3]Istinye University, Faculty of Pharmacy, Pharmaceutical Technology Department, Istanbul 34010, Türkiye

Abstract: *De novo* drug design has been studied utilizing the organic chemical structures of Salmon Calcitonin 9 - 19 and Peptide Nucleic Acid (PNA) to suppress Coronavirus Ribonucleic Acid (RNA)-Glycoprotein complex. PNA has a polyamide backbone and thymine pendant groups to bind and selectively inhibit adenine domains of the RNA-Glycoprotein complex. While doing so, molecular docking and molecular dynamics studies revealed that there is great inhibition docking energy (-12.1 kcal/mol) with significantly good inhibition constant (124.1 µM) values confirming the efficient nucleotide-specific silencing of Coronavirus RNA-Glycoprotein complex.

1. INTRODUCTION

A widespread disease emerged in December 2019 and caused a major health problem worldwide after its sudden strike in China (1-3). SARS-CoV-2, also known as the novel coronavirus, is the human pathogen that caused a global pandemic with well over 100,000 diagnosed patients across the world, from China to Europe and all the way to the U.S.A., and yet still, there is no efficient halt to this spread currently. There is now quite an effort within the industrial and scientific community to find an inhibition mechanism for SARS-CoV-2 via varying strategies to save millions of lives (4-8). There are far more than 350 genome sequences of SARS-CoV-2; however, 30,000 base-pair genomes of SARS-CoV-2 is quite a different strain from SARS-CoV which was a beta coronavirus infecting mankind that caused a major health problem in 2003 and 2004 (9,10).

Under these terms, especially in silico drug discovery and drug repurposing settings have become rapidly even more popular than they used to be and are utilized quite often since the beginning of this disease. SARS-CoV-2 enters into the human host cells through its spike subunit S1's binding to the host cell's ACE2 transport protein. The modulation of the spike S1 protein (which is bound to S2 protein where it is attached to the surface membrane SARS-CoV-2) occurs in such a way that its trimeric structure accepts homodimer ACE2 proteins, and the binding occurs in Figure 1. ACE2 is a type 1 membrane protein known to be highly expressed within the respiratory cells. The S1 is known to be an excellent cell surface receptor binder in terms of binding affinity and efficiency. Specific anti-viral drugs from pharmaceutical synthetic and pharmacological origins are being re-examined in terms of their binding mechanisms to the ACE-2 enzyme and S1 subunit protein of coronavirus. Several drugs are being used together in the patients currently instead of solely using a drug to be able to keep them alive. Chloroquine, Arbidol, Favipiravir, Remdesivir, and an anti-asthmatic drug, Zafirlukast, and several other antibiotics and antifungal drugs Itrazol, Fazadinium, Troglitazone, Gliquidone, Idarubicin, and Oxacillin are also being tested in clinical trials effective immediately. Sending spike proteins (S1 analogs) as the drug to bind them to ACE2 receptors was the first strategy, Figure 2a, in hand. Since these spike

protein analogs will block all ACE2 receptors, SAR-CoV-2 cannot bind to any ACE2. Thus, there will be no viral infection, and the immune system will be able to recognize these non-harmful spike proteins and develop a response to the SAR-CoV-2 in time. However, blocking a protein channel such as ACE2 might cause some side effects. In Figure 2b, scientists also thought of a similar approach. Utilizing antibodies instead of the spike proteins would yield a similar outcome since the outcome of permanently blocking all ACE2 receptors might have adverse side effects for the patients in the long run (11-13). According to Figure 2c, sending an inhibitory protein or drug such as Favipiravir to inhibit the S1 domains of SAR-CoV-2 directly might be an efficient route. With the spike proteins on the SAR-CoV-2 surface blocked, they can no longer get into interaction with ACE2 receptors (14).
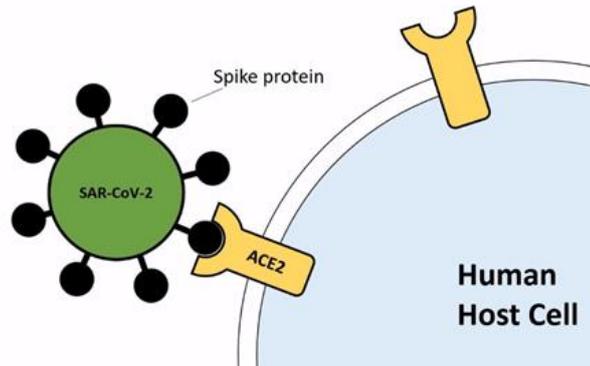

Figure 1: The binding illustration of the S1 subunit spike protein of SAR-CoV-2 and ACE2 transport protein of human host cell.

Nanobodies, also known as therapeutic antibodies, can serve the same purpose as stated in Figure 2d. A further advantage of these might be the choice of DNA sequences within the nanobodies. The choice of sequence might be beneficial for further intra-cellular mechanisms from the immune system perspective and aid in initiating the neutralizing immune response (15-17).

Rather than choosing these strategies to suppress coronavirus activity as the other scientists tried within the scientific literature, a significant de novo design (strategy Figure 3) was made via the complex of Calcitonin and Peptide Nucleic Acids (PNA) since the Calcitonin domain is essential for blood circulatory system bioavailability. In contrast, PNAs can be used to silence virus RNAs. Thus, the significance of Calcitonin and PNA should be mentioned. Calcitonin, a 32-amino-acid peptide, is secreted by the C-cells of the thyroid in mammals and by the ultimobranchial glands in sub-mammals. As a therapeutic agent for metabolic bone disease, Salmon calcitonin (SCT) has been in use for over three decades, and it has received approval for the treatment of postmenopausal osteoporosis in more than 90 countries. It is also approved for other indications such as Paget's disease, bone-associated pain conditions, and emergency treatment of hypercalcemia using injectable salmon calcitonin. The hormone's bioavailability within the bloodstream plays a crucial role in its mechanism. Initially identified in 1961 for its blood calcium-lowering properties, synthetic or recombinant Calcitonins from various species, including human, porcine, eel-derived, and SCT, have been employed for medical purposes. Over the past 15 years, new insights have emerged regarding the effects of SCT in preserving bone quality, particularly trabecular microarchitecture, which may contribute to its anti-fracture efficacy. SCT is the most widely used preparation in clinical practice, owing to its 40-50 times higher intrinsic potency compared to human calcitonin and its improved analgesic properties. Nonetheless, despite being discovered 45 years ago, the physiological role of calcitonin remains not entirely understood and continues to be the subject of ongoing research (18-24).

Peptide Nucleic Acids (PNAs) were originally designed as DNA-binding agents that target the major groove domain of DNA, similar to triplex-forming oligonucleotides. Instead of using the sugar-phosphate backbone found in oligonucleotides, PNAs were created with a pseudopeptide backbone (25). Upon synthesis, it became evident that PNAs, with their backbone and nucleobase linkers, closely mimic the structure of DNA and RNA. They can form stable duplex structures with complementary DNA, RNA, or other PNA oligomers (26-28). The synthesis of PNA oligomers can be done through standard solid-phase manual or automated peptide synthesis, using either tBoc or Fmoc-protected PNA monomers (29-31). After synthesis, the oligomers are deprotected and separated from the polymer using TFMSA/TFA (for tBoc) or purified through reversed-phase HPLC. Characterization of the oligomers can be done using MALDI-TOF or proton NMR. PNA oligomers can be easily labeled with fluorophores or biotin. In cellular uptake experiments conducted in vitro and in vivo, PNA oligomers are used as antisense or antigen agents, typically consisting of 12-18 nucleobases and having molecular weights of 3000-4000 amu. These hydrophilic structures have applications as antigens, antibacterial, and antiviral agents. These oligomers demonstrated intriguing characteristics in a complex formed by the interaction of polyamide nucleic acid with purine and pyrimidine bases

attached to it. Notably, they exhibit high stability in human serum and cell extracts and exhibit

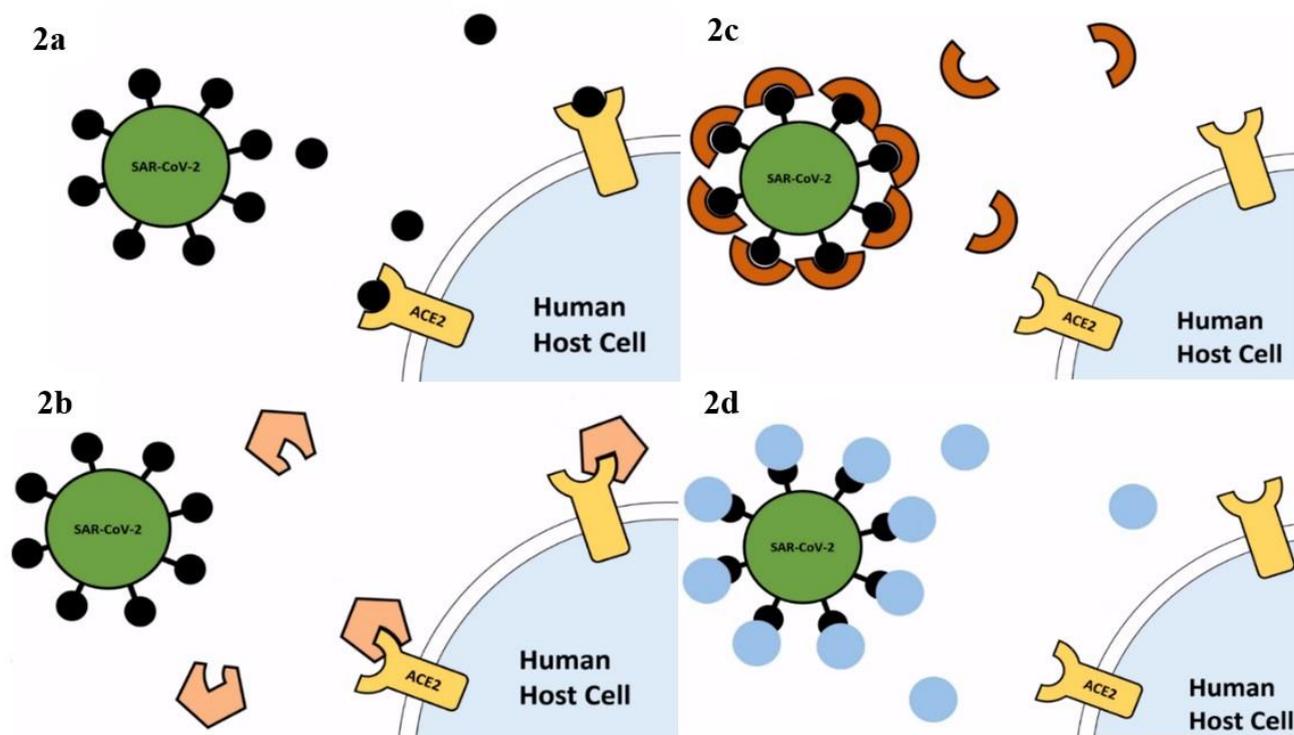antisense activity and suppress HIV virus RNA (32-37).

Figure 2: Strategy 2a: Occupying the ACE2 Receptors with ACE2 binding drugs (spike proteins); Strategy 2b: Occupying the ACE2 Receptors with ACE2 binding drugs (antibodies); Strategy 2c: Blocking SAR-CoV-2 directly via inhibitory drugs; Strategy 2d: Blocking SAR-CoV-2 directly via nanobodies.

Hence, studying the antiviral complementary suppression activity of Polyamide-backboned PNA combined with the superior bioavailability features of SCT is the primary goal of this research paper. For the sake of argument, we can call our designed ligand (drug) Peptide Polyamide Nucleic Acid complexed with Salmon Ligand, or in short, PPNASL, which will serve as an Adenine binder and inhibitor of RNA of Coronavirus along with its attached Glycoprotein.

2. MATERIALS AND METHODS

2.1. Geometric Optimization
An accurate determination of its geometrically optimal structure is essential to determine the active sites of any molecule and investigate its interactions with receptors. In our current study, the ligand designed to inhibit Coronavirus RNA-glycoprotein was determined using our group's vast organic/pharmaceutical chemistry knowledge. These organic chemical structures, with their most stable molecular geometries, went under the processing of the Gaussian 09 software (38) with density functional theory (DFT)/B3LYP functional (39). Using the 6-31G(d,p) principle, the most stable molecular structures of polyamide-g-thymine and calcium molecules were formed for computational and simulation further research, as can be seen in

Figure 1. GaussView 6.0 and Avogadro 1.95 software (40) was used to prepare the input files for the molecular docking and molecular dynamics computations as well as for the post-processing of the output files.

2.2. Molecular Docking Procedure
All molecular docking simulations were performed via AutoDock Vina 1.1.2. and PyRx 0.8 software (41), both of which are widely used and accepted for their great precision and accuracy in biochemical docking simulations. The docking simulations took 50 posed simulations to 100 posed simulations in each run, totaling 800 poses. The drug complex of PPNASL has two domains. Its PNA (Polyamide-g-Thymine) part was de novo designed. In contrast, its Calcitonin part, along with the receptor structure of Coronavirus RNA-Glycoprotein, was downloaded from the Zinc Database with the following IDs of 2GLG and 7ACT, respectively. The optimizations were done using Gauss View 6.0 and Avogadro 1.95 and run, illustrating the interaction and binding of the drug to the receptor. The docking scores of all simulations were in kcal/mol as units stating the Gibbs free binding energy. The docking poses with the most accurate and favorable binding energy within the best-clustered data were chosen to be used as the initial structure and input file for MD simulations in each simulation with different seed numbers.

2.3. Molecular Dynamics (MD) Simulations

The docking poses possessing the best and most favorable binding energy concerning the docking results were used as the initial structure for the MD simulations (42,43). Utilizing Schrödinger's Maestro Desmond software (44), all the ligands were run for molecular dynamics (MD) simulations with 50 ns total time periods per each new seeded run, including 5000 poses with 10 ps time intervals, respectively. Each molecular dynamics simulation was repeated 3 times with different seed numbers to ensure the simulation parameters and structure of the PPNASL (ligand) bound Coronavirus RNA-Glycoprotein (receptor) complexes were correct. MD simulations were run to evaluate the dynamic properties of the drug-receptor complexes over time. The grid box in which the system was created was set to $150 \times 150 \times 150 \text{ Å}^3$ and with the spacing of 0.5 Å choice for this large receptor. TIP3P-type water molecules were placed in the box, and 0.15 M NaCl ions were also added to neutralize the system. As the temperature and pressure parameters, NPT was employed at 310 K with Nose-Hoover temperature coupling (45) and at the constant pressure of 1.01 bar via Martyna Tobias−Klein pressure coupling (46). There were not any constraints on the systems, and the initial velocity values for the force field calculations were used as default fitting for OPLS 3.0 standards.

2.4. Post Molecular Dynamics Characterizations

The trajectory datasets of MD results were used for ''Hydrogen contact mapping analyses'' so that atom by atom, the complexes' binding effects and the drug's efficiency could be verified. The ''Event Analyses'' modules of Schrödinger's Maestro Desmond software were used for this purpose, where these results can be compared to the inhibition constant values.

3.   RESULTS AND DISCUSSION

To achieve the goal of suppressing the activity of Coronavirus RNA-Glycoprotein by silencing its RNA to block its expression, one should know the pharmaceutical chemistry tendencies of functional groups and the genetic engineering aspects of the nucleotide-specific silencing on the receptors and its bioactivity features. The effectiveness of interactions appears to depend on various factors, including the affinity of the drug's pendant Thymine domains to RNA and the topology of the binding.

In our strategy to suppress Coronavirus, shown in Figure 3, the organic chemical structure of the designed drug (ligand) can be seen at pH 7.4. By merging PNA (Polyamide-g-Thymine) with Salmon Calcitonin 9-19, the efficiency of the ligand was planned to be increased in terms of chemical Hydrogen bond affinity towards the receptor since the mode of binding and the nucleotide regioselectivity plays a pivotal role in the inhibition and suppression mechanism.

Triple Thymine groups were chosen to bind to the Adenine groups of Coronavirus RNA-Glycoprotein, which has multiple repeating Adenines. This PNA oligomer possessing a Polyamide backbone with Thymine grafts is especially the right fit for the job in terms of RNA silencing (37, 48-50). For the first time here, we use it to silence Coronavirus RNA.
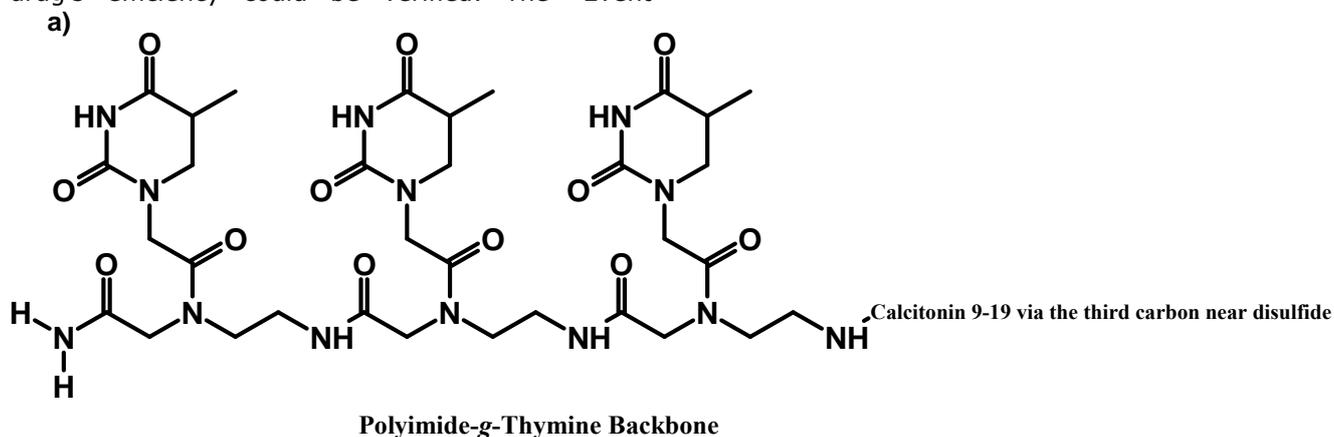
a)

Polyimide-*g*-Thymine Backbone

Figure 3: The de novo drug's chemical structure.

The second issue that should be referred to is that in terms of pharmacokinetics, the addition of Calcitonin to the ligand structure is significantly beneficial due to its good bioavailability within the blood circulatory system. In our *in silico* studies, referring to a published research paper of the Ph.D. thesis (51) of our group, which had the experimental in vitro and in vivo findings, the half-life of Calcitonin had the range of 50 to 80 minutes while its protein binding rate is 30-40%. Due to its peptide-based structure, Calcitonin is easily broken down in the gastrointestinal tract. Hence, it can be administered parenterally or intranasally. The plasma concentrations of 0.1-0.4 ng/mL were obtained after 200 units of subcutaneous administration. While there is an immediate effect after intravenous administration, the effect is observed 15 minutes after intramuscular or subcutaneous administration. Salmon Calcitonin has the greatest effect approximately 4 hours after intramuscular or subcutaneous administration. While the effect after intravenous administration lasts between 30 minutes and 12 hours, it lasts for

about 8-24 hours after intramuscular and subcutaneous administration.

In Figure 4, the organic chemical structure of the receptor target, Coronavirus RNA-Glycoprotein, is illustrated. Since the glycoprotein and RNA domains are merged within the nuclei of Coronaviruses, it is best to study the inhibition of the whole complex.
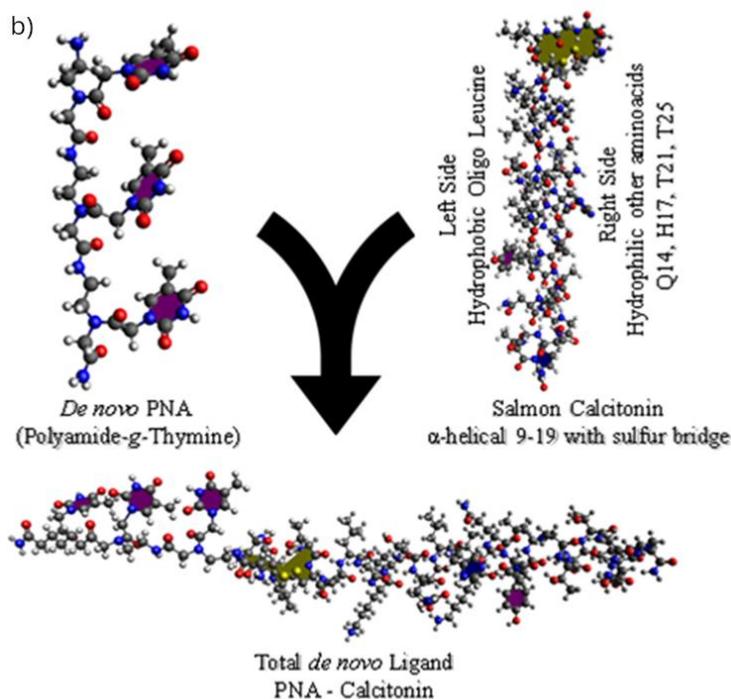

Figure 4: a) Chemical structure of PPNASL. b) *De novo* strategy for designing the biochemical organic structure of PPNASL.
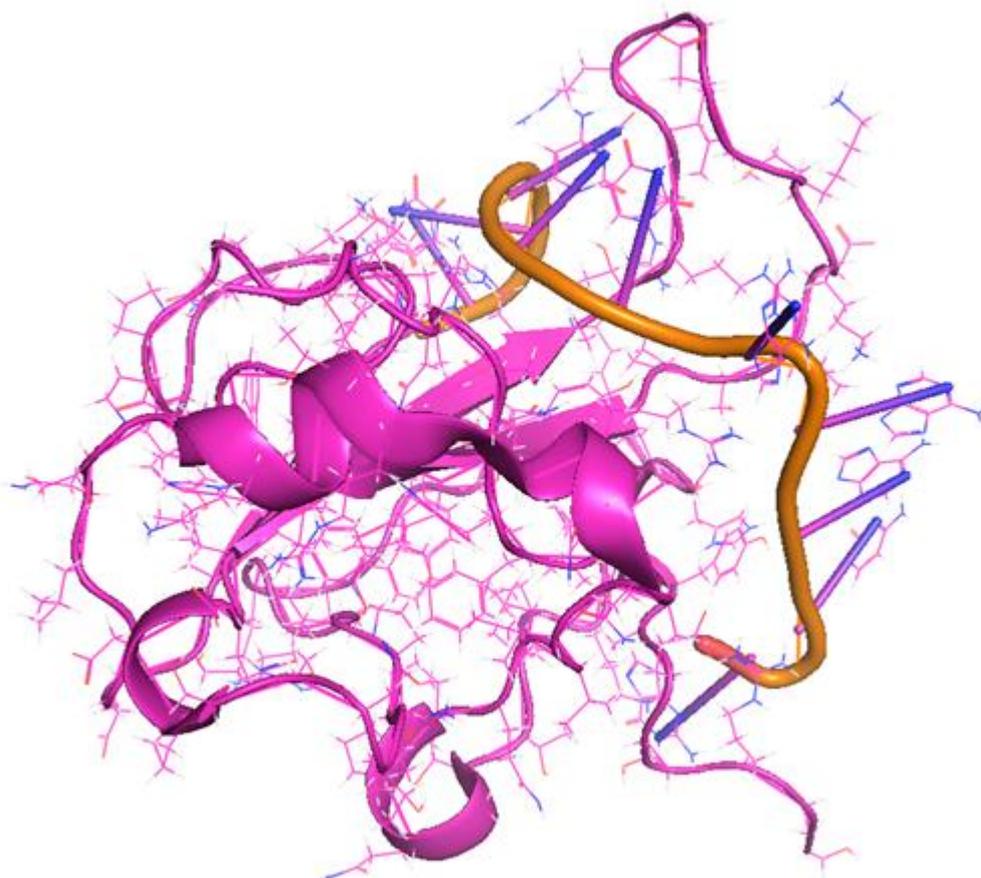

Figure 5: The receptor molecule: 3-D chemical structure of Coronavirus RNA-Glycoprotein.

The 3-D chemical structure of Coronavirus RNA-Glycoprotein was optimized using Gauss view and Avogadro. It was seen that the steric hindrance of RNA is not as much as one can expect, which is a good starting point. Since its nucleotides, especially recurring Adenine triplets, are exposed, and the Polyamide-g-Thymine triplets of PPNASL can find the affinity and availability towards these sites easily and docks onto them efficiently with Δ(ΔG) of -12.1 kcal/mol and significantly good inhibition constant of 124.1 µM.

By simulating and computing the theoretical stability and binding energies of PPNASL docked onto Coronavirus RNA-Glycoprotein, Figure 6 illustrates one of the main poses of the PPNASL, taken under 3D video within Schrodinger's Maestro Desmond MD software, where the MD run had 5000 frames. The thymine pendant groups on polyamide PNA selectively chose the adenine triplet of coronavirus RNA and silenced it.

Another detailed close-up shot of the docked pose of the ligand to Coronavirus RNA can be seen Ligand-receptor complex equilibrium and stabilization occur in Figure 7. The Thymine-Adenine binding of the ligand-receptor complex can be observed clearly.
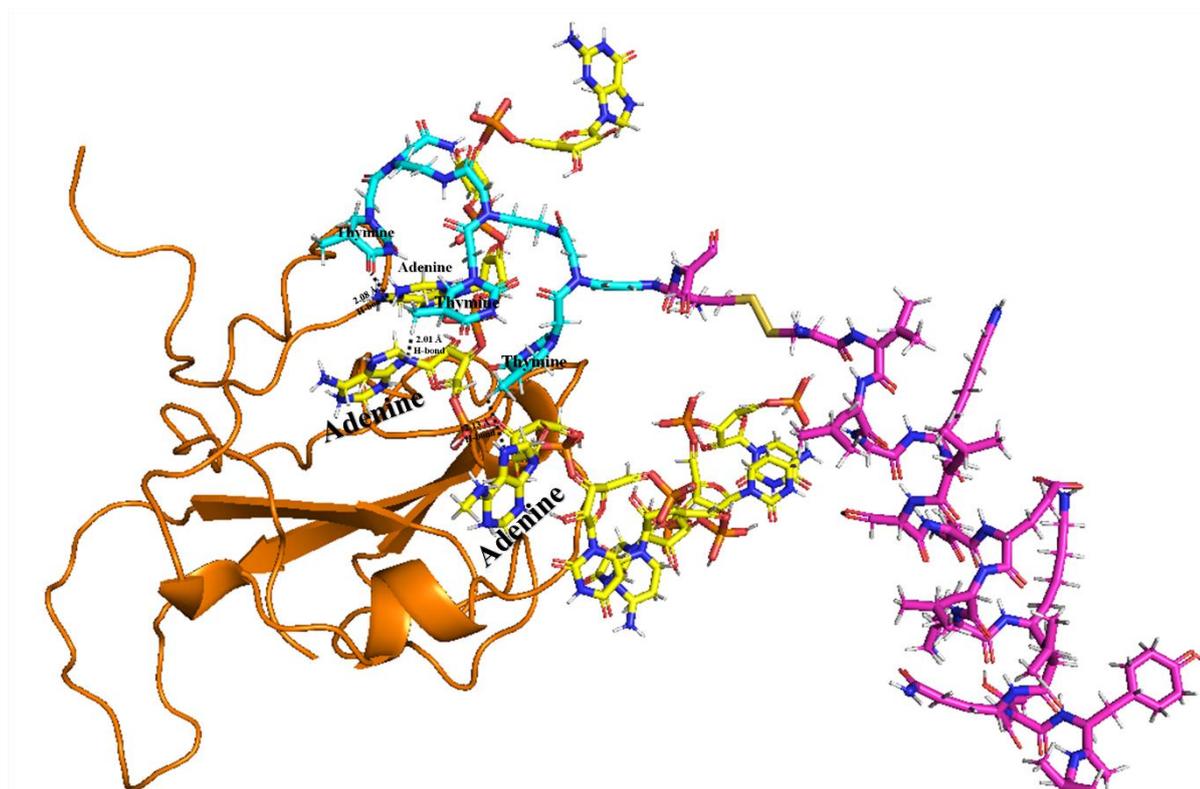

Figure 6: The best favored MD pose of PPNASL docked onto Coronavirus RNA-Glycoprotein.

Table 1: The Post-Molecular Dynamics Hydrogen bond contact mapping analyses of PPNASL

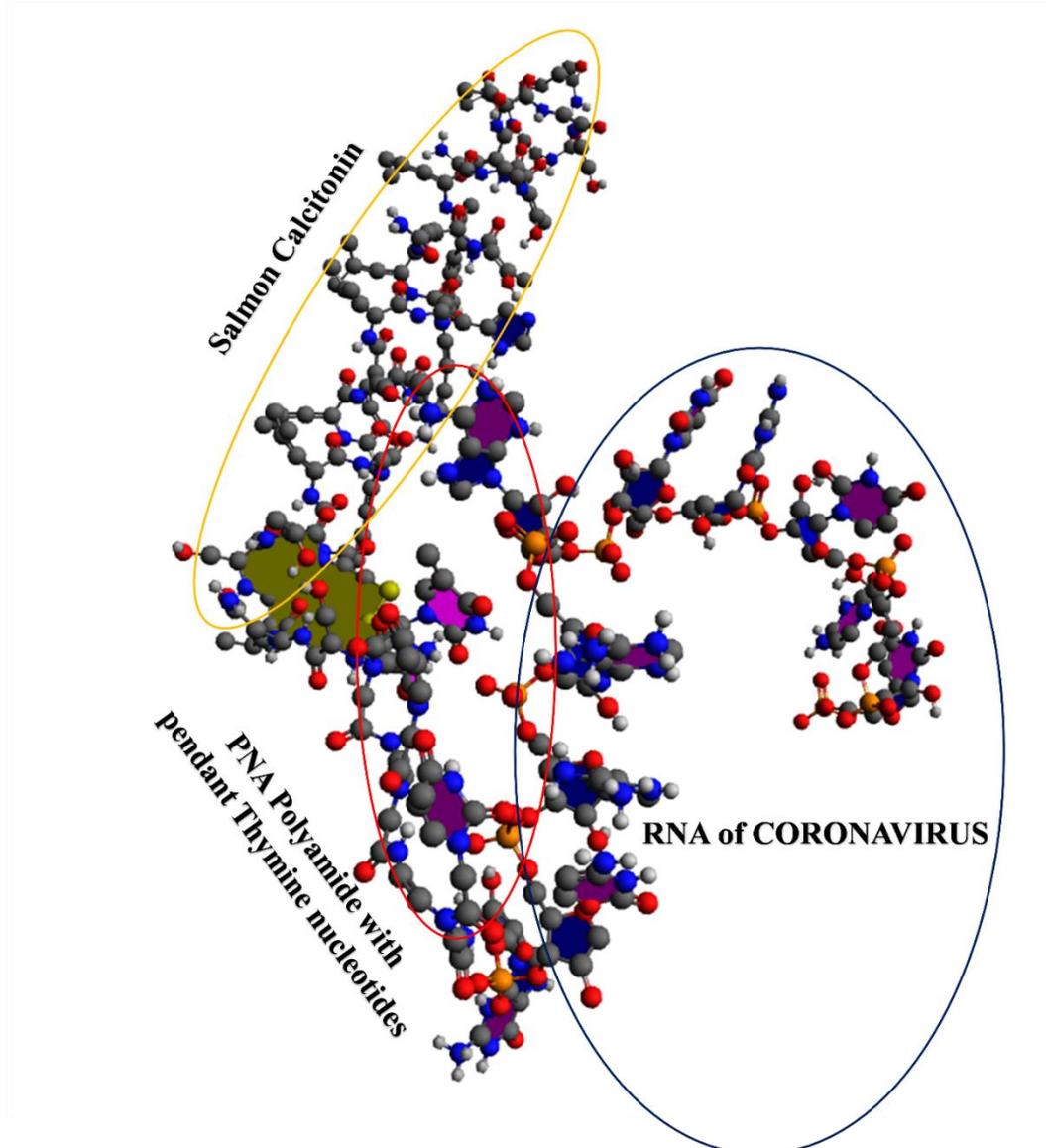| RNA domains	% of H-Bonds Thymines choose RNA	Binding Energy (kcal/mol)	H-Bond Distance (Å)
Adenine (1)	30.4	-12.4	2.08
Adenine (2)	32.3	-11.9	2.01
Adenine (3)	31.8	-12.0	2.13
The Rest	5.5	-	-

Figure 7: The close-up shot of the best favored MD pose of PPNASL docked onto Coronavirus RNA.

After conducting 3D motion trajectory analyses, Table 1 presents a subsequent investigation using Schrödinger Maestro Desmond's Event Analyses tools. The aim was to compute all potential interactions between functional groups on drugs and RNA domains. This intricate affinity and binding study involved examining all hydrogen bonds among thousands of atoms based on the matrix data from the MD study's trajectory files.

Matrix matches were manually performed for each atom to analyze the post-MD Hydrogen contact mapping. Additionally, a machine learning pre-coded script was utilized to determine the regioselectivity of Thymine groups of Polyamide PNA towards the Adenine domains of RNA. This approach was adopted to calculate the percentages of tendencies for functional group bindings.

The drug aligns and maneuvers itself onto the Adenine domains regioselectively, and strong Hydrogen forces (2.08, 2.01, 2.13 Å) take place there, maintaining inhibitory $\Delta(\Delta G)$ energies (-12.4, 11.9, -12.0 kcal/mol) so that PPNASL suppresses the RNA-Glycoprotein activity.

In Figure 8, it can be seen that after around 30 nanoseconds, the whole complex begins to reach an equilibrium in the yellow color compared to the non-bound pristine receptor (target molecule) of Coronavirus RNA, indicating lower oscillations and a stable structure form in the ligand-receptor bound situation. However, as can be seen from the blue Coronavirus RNA illustration, the oscillations among the atoms of the RNA structure go on around 2Å and do not diminish.
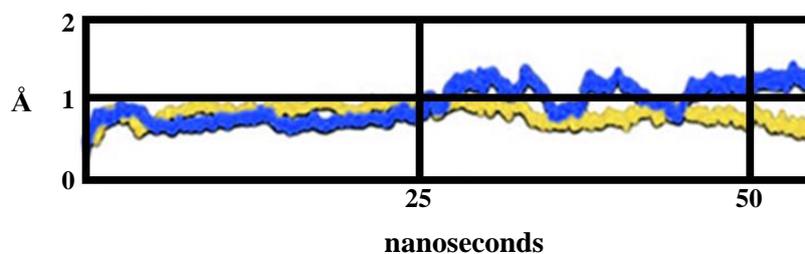
Figure 8: The Root Mean Square Deviation plot (R.M.S.D.) of all atoms studied under the force field of OPLS 3.0; PNA-Thymine in complex with RNA in yellow and non-bound receptor Coronavirus RNA (pristine) in blue respectively.

4.   CONCLUSIONS

This research study has explored de novo drug design methods by utilizing the organic chemical structures of Salmon Calcitonin 9 - 19 and PNA to target the Coronavirus Ribonucleic Acid (RNA)-Glycoprotein complex. PNA, with its polyamide backbone and Thymine pendant groups, has been employed to selectively bind and inhibit the Adenine domains of the RNA-glycoprotein complex. Molecular docking, molecular dynamics, and post-MD characterization studies were conducted, revealing a highly favorable inhibition total docking energy of -12.1 kcal/mol and a significantly good inhibition constant of 124.1 μM. These findings confirm the effective and regioselective suppression of the Coronavirus RNA-Glycoprotein complex at the nucleotide level. This also proves the achievement of the Molecular Dynamics

5.   CREDIT AUTHORSHIP CONTRIBUTION STATEMENT

Soykan Agar, Ph.D.: Computer-Aided Drug Design, Computational Experimenting and Writing the original draft and full paper. Barbaros Akkurt, Ph.D.: Writing the original draft and full paper, proofreading. Levent Alparslan, Ph.D.: Investigation, Supervision.

6. DECLARATION OF COMPETING INTEREST

The authors declare that they have no known competing financial interests or personal relationships that could have appeared to influence the work reported in this paper.

7. DATA AVAILABILITY

Data will be made available on request.

8. REFERENCES

1. Dong L, Hu S, Gao J. Discovering drugs to treat coronavirus disease 2019 (COVID-19). DD&T. 2020 Feb 29;14(1):58–60. Available from: <DOI>.

2. Commission NH, others. Guidelines for the Prevention, Diagnosis, and Treatment of Novel Coronavirus-Induced Pneumonia. National Health Commission, Beijing, China,; 2020.

3. Jin Z, Du X, Xu Y, Deng Y, Liu M, Zhao Y, et al. Structure of M pro from COVID-19 virus and discovery of its inhibitors [Internet]. Biochemistry; 2020 Feb [cited 2023 Nov 7]. Available from: <DOI>.

4. Senathilake K, Samarakoon S, Tennekoon K. Virtual Screening of Inhibitors Against Spike Glycoprotein of SARS-CoV-2: A Drug Repurposing Approach [Internet]. LIFE SCIENCES; 2020 Mar [cited 2023 Nov 7]. Available from: <DOI>.

5. Chan JFW, Yuan S, Kok KH, To KKW, Chu H, Yang J, et al. A familial cluster of pneumonia associated with the 2019 novel coronavirus indicating person-to-person transmission: a study of a family cluster. The Lancet. 2020 Feb;395(10223):514–23. Available from: <DOI>.

6. Lu R, Zhao X, Li J, Niu P, Yang B, Wu H, et al. Genomic characterisation and epidemiology of 2019 novel coronavirus: implications for virus origins and receptor binding. The Lancet. 2020 Feb;395(10224):565–74. Available from: <DOI>.

7. Liu C, Zhou Q, Li Y, Garner LV, Watkins SP, Carter LJ, et al. Research and Development on Therapeutic Agents and Vaccines for COVID-19 and Related Human Coronavirus Diseases. ACS Cent Sci. 2020 Mar 25;6(3):315–31. Available from: <DOI>.

8. Wan Y, Shang J, Graham R, Baric RS, Li F. Receptor Recognition by the Novel Coronavirus from Wuhan: an Analysis Based on Decade-Long Structural Studies of SARS Coronavirus. Gallagher T, editor. J Virol. 2020 Mar 17;94(7):e00127-20. Available from: <DOI>.

9. Xu X, Chen P, Wang J, Feng J, Zhou H, Li X, et al. Evolution of the novel coronavirus from the ongoing Wuhan outbreak and modeling of its spike protein for risk of human transmission. Sci China Life Sci. 2020 Mar;63(3):457–60. Available from: <DOI>.

10. Huentelman MJ, Zubcevic J, Hernández Prada JA, Xiao X, Dimitrov DS, Raizada MK, et al. Structure-Based Discovery of a Novel Angiotensin-Converting Enzyme 2 Inhibitor. Hypertension. 2004 Dec;44(6):903–6. Available from: <DOI>.

11. Khaerunnisa S, Kurniawan H, Awaluddin R, Suhartati S, Soetjipto S. Potential Inhibitor of COVID-19 Main Protease (Mpro) From Several Medicinal Plant Compounds by Molecular Docking Study [Internet]. MEDICINE & PHARMACOLOGY; 2020 Mar [cited 2023 Nov 7]. Available from: <DOI>.

12. Chang KO, Kim Y, Lovell S, Rathnayake A, Groutas W. Antiviral Drug Discovery: Norovirus Proteases and Development of Inhibitors. Viruses. 2019 Feb 25;11(2):197. Available from: <DOI>.

13. Li JY, You Z, Wang Q, Zhou ZJ, Qiu Y, Luo R, et al. The epidemic of 2019-novel-coronavirus (2019-nCoV) pneumonia and insights for emerging infectious diseases in

the future. Microbes and Infection. 2020 Mar;22(2):80–5. Available from: <DOI>.

14. Delang L, Abdelnabi R, Neyts J. Favipiravir as a potential countermeasure against neglected and emerging RNA viruses. Antiviral Research. 2018 May;153:85–94. Available from: <DOI>.

15. Xu Z, Peng C, Shi Y, Zhu Z, Mu K, Wang X, et al. Nelfinavir was predicted to be a potential inhibitor of 2019-nCov main protease by an integrative approach combining homology modelling, molecular docking and binding free energy calculation [Internet]. Pharmacology and Toxicology; 2020 Jan [cited 2023 Nov 7]. Available from: <DOI>.

16. Gopal Samy B, Xavier L. Molecular docking studies on antiviral drugs for SARS. International Journal. 2015;5(3):75–9.

17. Peng C, Zhu Z, Shi Y, Wang X, Mu K, Yang Y, et al. Computational study of the strong binding mechanism of SARS-CoV-2 spike and ACE2 [Internet]. Chemistry; 2020 Feb [cited 2023 Feb 22]. Available from: <DOI>.

18. Copp DH, Cameron EC. Demonstration of a Hypocalcemic Factor (Calcitonin) in Commercial Parathyroid Extract. Science. 1961 Dec 22;134(3495):2038–2038. Available from: <DOI>.

19. Azria M, Copp DH, Zanelli JM. 25 Years of salmon calcitonin: From synthesis to therapeutic use. Calcif Tissue Int. 1995 Dec;57(6):405–8. Available from: <DOI>.

20. Woodrow J, Noseworthy C, Fudge N, Hoff A, Gagel R, Kovacs C. Calcitonin/calcitonin gene-related peptide protect the maternal skeleton from excessive resorption during lactation. Journal of bone and mineral research. 2003. p. S37–S37.

21. Hoff A, Thomas P, Cote G, Qiu H, Bain S, Puerner D, et al. Generation of a calcitonin knockout mouse model. Bone. 1998;23(suppl 5):S164.

22. Hirsch PF, Baruch H. Is Calcitonin an Important Physiological Substance? ENDO. 2003;21(3):201–8. Available from: <DOI>.

23. Hoff AO, Catala-Lehnen P, Thomas PM, Priemel M, Rueger JM, Nasonkin I, et al. Increased bone mass is an unexpected phenotype associated with deletion of the calcitonin gene. J Clin Invest. 2002 Dec 15;110(12):1849–57. Available from: <DOI>.

24. Zaidi M, Inzerillo AM, Troen B, Moonga BS, Abe E, Burckhardt P. Molecular and Clinical Pharmacology of Calcitonin. In: Principles of Bone Biology [Internet]. Elsevier; 2002 [cited 2023 Nov 7]. p. 1423–40. Available from: <DOI>.

25. Nielsen PE, Egholm M, Berg RH, Buchardt O. Sequence-Selective Recognition of DNA by Strand Displacement with a Thymine-Substituted Polyamide. Science. 1991 Dec 6;254(5037):1497–500. Available from: <DOI>.

26. Wittung P, Nielsen PE, Buchardt O, Egholm M, Nordén B. DNA-like double helix formed by peptide nucleic acid. Nature. 1994 Apr;368(6471):561–3. Available from: <DOI>.

27. Jensen KK, Ørum H, Nielsen PE, Nordén B. Kinetics for Hybridization of Peptide Nucleic Acids (PNA) with DNA and RNA Studied with the BIAcore Technique. Biochemistry. 1997 Apr 1;36(16):5072–7. Available from: <DOI>.

28. Egholm M, Buchardt O, Christensen L, Behrens C, Freier SM, Driver DA, et al. PNA hybridizes to complementary oligonucleotides obeying the Watson–Crick hydrogen-bonding rules. Nature. 1993 Oct;365(6446):566–8. Available from: <DOI>.

29. Christensen L, Fitzpatrick R, Gildea B, Petersen KH, Hansen HF, Koch T, et al. Solid-Phase synthesis of peptide nucleic acids. Journal of Peptide Science. 1995 May;1(3):175–83. Available from: <DOI>.

30. Dueholm KL, Egholm M, Behrens C, Christensen L, Hansen HF, Vulpius T, et al. Synthesis of peptide nucleic acid monomers containing the four natural nucleobases: thymine, cytosine, adenine, and guanine and their oligomerization. The Journal of Organic Chemistry. 1994;59(19):5767–73. Available from: <DOI>.

31. Thomson SA, Josey JA, Cadilla R, Gaul MD, Fred Hassman C, Luzzio MJ, et al. Fmoc mediated synthesis of Peptide Nucleic Acids. Tetrahedron. 1995 May;51(22):6179–94. Available from: <DOI>.

32. N. Ganesh K, E. Nielsen P. Peptide Nucleic Acids: Analogs and Derivatives. Current Organic Chemistry. 2000 Sep 1;4(9):931–43. Available from: <DOI>.

33. Eldrup AB, Dahl O, Nielsen PE. A Novel Peptide Nucleic Acid Monomer for Recognition of Thymine in Triple-Helix Structures. J Am Chem Soc. 1997 Nov 1;119(45):11116–7. Available from: <DOI>.

34. Ljungstrøm T, Knudsen H, Nielsen PE. Cellular Uptake of Adamantyl Conjugated Peptide Nucleic Acids. Bioconjugate Chem. 1999 Nov 1;10(6):965–72. Available from: <DOI>.

35. Cutrona G, Carpaneto EM, Ulivi M, Roncella S, Landt O, Ferrarini M, et al. Effects in live cells of a c-myc anti-gene PNA linked to a nuclear localization signal. Nat Biotechnol. 2000 Mar;18(3):300–3. Available from: <DOI>.

36. Mologni L. Additive antisense effects of different PNAs on the in vitro translation of the PML/RARalpha gene. Nucleic Acids Research. 1998 Apr 15;26(8):1934–8. Available from: <DOI>.

37. Mayhood T, Kaushik N, Pandey PK, Kashanchi F, Deng L, Pandey VN. Inhibition of Tat-Mediated Transactivation of HIV-1 LTR Transcription by Polyamide Nucleic Acid Targeted to TAR Hairpin Element. Biochemistry. 2000 Sep 1;39(38):11532–9. Available from: <DOI>.

38. Frisch MJ, Trucks GW, Schlegel HB, Scuseria GE, Robb MA, Cheeseman JR, et al. Gaussian 09, Revision D.01. Wallingford, CT: Gaussian, Inc.; 2009.

39. Becke A. Density-Functional Thermochemistry. III. The Role of Exact Exchange. J Chem Phys. 1993;98:5648–52.

40. Dennington R, Keith TA, Millam JM. GaussView 5.0. Wallingford, CT: Gaussian, Inc.; 2009.

41. Gaillard T. Evaluation of AutoDock and AutoDock Vina on the CASF-2013 Benchmark. J Chem Inf Model. 2018 Aug 27;58(8):1697–706. Available from: <DOI>.

42. Şenel P, Agar S, İş YS, Altay F, Gölcü A, Yurtsever M. Deciphering the mechanism and binding interactions of Pemetrexed with dsDNA with DNA-targeted chemotherapeutics via spectroscopic, analytical, and simulation studies. Journal of Pharmaceutical and Biomedical Analysis. 2022 Feb;209:114490. Available from: <DOI>.

43. Cheraghi S, Şenel P, Dogan Topal B, Agar S, Majidian M, Yurtsever M, et al. Elucidation of DNA-Eltrombopag Binding: Electrochemical, Spectroscopic and Molecular Docking Techniques. Biosensors. 2023 Feb 21;13(3):300. Available from: <DOI>.

44. Desmond D. Shaw Research: New York. NY; 2017.

45. Evans DJ, Holian BL. The Nose–Hoover thermostat. The Journal of Chemical Physics. 1985 Oct 15;83(8):4069–74. Available from: <DOI>.

46. Martyna GJ, Tobias DJ, Klein ML. Constant pressure molecular dynamics algorithms. The Journal of Chemical Physics. 1994 Sep 1;101(5):4177–89. Available from: <DOI>.

47. Mestre B, Arzumanov A, Singh M, Boulmé F, Litvak S, Gait MJ. Oligonucleotide inhibition of the interaction of HIV-1 Tat protein with the trans-activation responsive region (TAR) of HIV RNA. Biochimica et Biophysica Acta (BBA) - Gene Structure and Expression. 1999 Apr;1445(1):86–98. Available from: <DOI>.

48. Mhashilkar AM, Biswas DK, LaVecchio J, Pardee AB, Marasco WA. Inhibition of human immunodeficiency virus type 1 replication in vitro by a novel combination of anti-Tat single-chain intrabodies and NF-kappa B antagonists. J Virol. 1997 Sep;71(9):6486–94. Available from: <DOI>.

49. Hirschman SZ, Chen CW. Peptide nucleic acids stimulate gamma interferon and inhibit the replication of the human immunodeficiency virus. J Investig Med. 1996 Aug;44(6):347–51. Available from: <URL>.

50. Alparslan AL, Yildiz Türkyilmaz G, Kozaci LD, Karasulu E. Thermoreversible Gel Formulation for the Intranasal Delivery of Salmon Calcitonin and Comparison Studies of In Vivo Bioavailability. tjps. 2023 Jun 1;20(3):127–40. Available from: <DOI>.

51. Şenel P, Agar S, Sayin VO, Altay F, Yurtsever M, Gölcü A. Elucidation of binding interactions and mechanism of Fludarabine with dsDNA via multispectroscopic and molecular docking studies. Journal of Pharmaceutical and Biomedical Analysis. 2020 Feb;179:112994. Available from: <DOI>.